

A kinematically compatible framework for cooperative payload transport by nonholonomic mobile manipulators

M. Abou-Samah · C. P. Tang · R. M. Bhatt · V. Krovi

Received: 5 August 2005 / Revised: 25 May 2006 / Accepted: 30 May 2006 / Published online: 5 September 2006
© Springer Science + Business Media, LLC 2006

Abstract In this paper, we examine the development of a kinematically compatible control framework for a modular system of wheeled mobile manipulators that can team up to cooperatively transport a common payload. Each individually autonomous mobile manipulator consists of a differentially-driven Wheeled Mobile Robot (WMR) with a mounted two degree-of-freedom (d.o.f) revolute-jointed, planar and passive manipulator arm. The composite wheeled vehicle, formed by placing a payload at the end-effectors of two (or more) such mobile manipulators, has the capability to accommodate, detect and correct both instantaneous and finite relative configuration errors.

The kinematically-compatible motion-planning/control framework developed here is intended to facilitate maintenance of all kinematic (holonomic and nonholonomic) constraints within such systems. Given an arbitrary end-effector trajectory, each individual mobile-manipulator's bi-level hierarchical controller first generates a *kinematically-feasible desired trajectory* for the WMR base, which is then tracked by a suitable lower-level posture stabilizing controller. Two variants of system-level cooperative control schemes—leader-follower and decentralized control—

are then created based on the individual mobile-manipulator control scheme. Both methods are evaluated within an implementation framework that emphasizes both virtual prototyping (VP) and hardware-in-the-loop (HIL) experimentation. Simulation and experimental results of an example of a two-module system are used to highlight the capabilities of a real-time local sensor-based controller for accommodation, detection and correction of relative formation errors.

Keywords Composite system · Hardware-in-the-loop · Mobile manipulator · Physical cooperation · Redundancy resolution · Virtual prototyping

1 Introduction

Cooperation has been the key to success of most human endeavors and the similar incorporation of cooperation in robotic systems is critical to realize the next generation of systems and applications. Interest in cooperating systems arises when the tasks are inherently too complex for a single system to accomplish; or when building and using several simple systems can be more flexible, fault-tolerant or cheaper than using a single large system.

Our guiding vision is to create and evaluate an overall framework for cooperative payload transport using a fleet of semi-autonomous wheeled mobile manipulator modules. Within this framework we examine coupling of various modules to create a larger variable-topology composite-wheeled system, with inherent internal reconfigurability to accommodate disturbances and enhance payload manipulation capabilities. The proposed application arena ranges from industrial applications, where suitable numbers of such modules can be tasked to manipulate variable-sized payloads, to extra-terrestrial applications, where individual rover modules sent on separate missions can cooperate to support planetary

M. Abou-Samah
MSC Software Corporation,
Ann Arbor, MI 48105, USA
e-mail: gishm@hotmail.com

C. P. Tang · R. M. Bhatt · V. Krovi (✉)
Mechanical and Aerospace Engineering, State University of
New York at Buffalo, Buffalo, NY 14260, USA
e-mail: vkrovi@eng.buffalo.edu

C. P. Tang
e-mail: chintang@eng.buffalo.edu

R. M. Bhatt
e-mail: rmbhatt@eng.buffalo.edu

colonization efforts (Adams et al., 1996; Juberts, 2001; Schenker et al., 2000).

In our system, each basic module consists of a passive, planar, two degree-of-freedom (d.o.f.) revolute-jointed manipulator mounted on a differentially-driven Wheeled Mobile Robot (WMR), as shown in Fig. 1(a) and (c). An effective articulated compliant linkage between the wheeled bases is created when a common payload is placed on the end-effectors of multiple adjacent modules, as shown in Fig. 1(b) and (d). The resulting composite vehicle now possesses: (a) the ability to accommodate changes in the relative configuration (by virtue of the compliant linkage); (b) a mechanism for detecting such changes (using sensed articulations); and (c) means to compensate for such disturbances (using the redundant actuation of the bases), while performing the payload transport task.

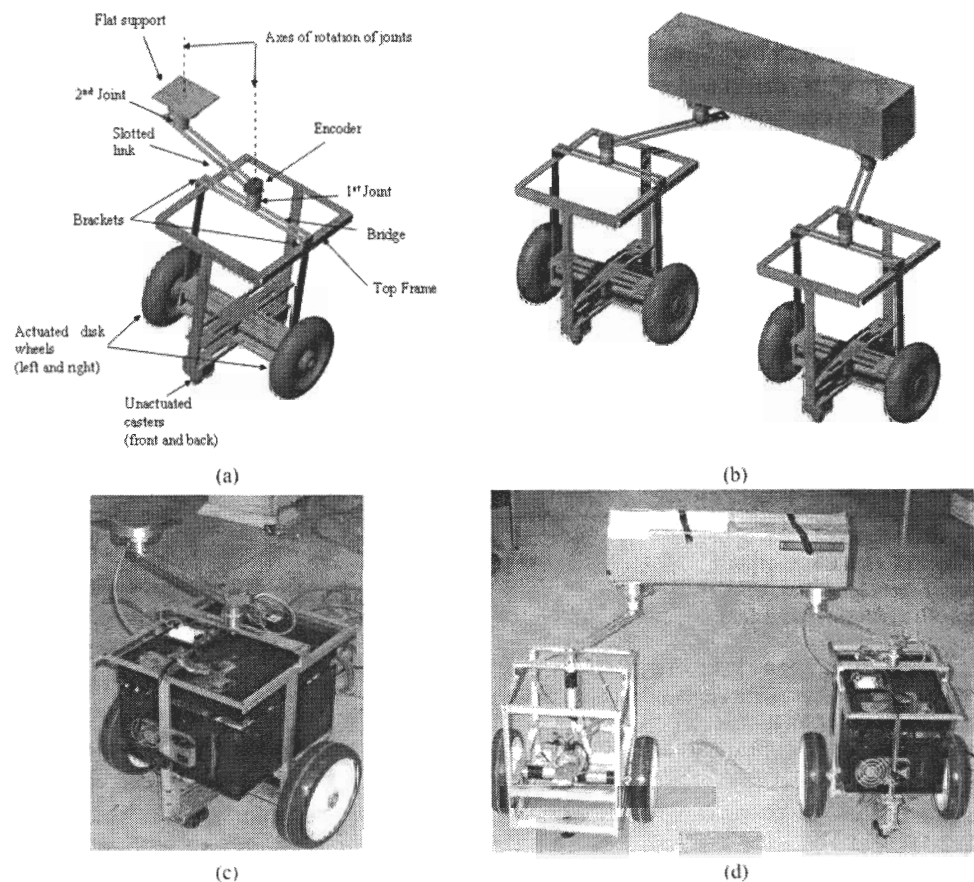
1.1 Background

Over the millennia, wheeled platform designs (with multiple sets of disc wheels attached to a common chassis) have remained popular in payload transport applications since they permit the load and traction forces to be distributed between the multiple wheels. However, the mobility, steerability, and controllability of the overall wheeled system depend largely

upon the type, nature and locations of the attached wheels. The process of *selecting* and *attaching* the set of wheels in a multiple-wheeled system creates various kinematic (holonomic/nonholonomic) compatibility constraints. Arbitrarily actuating such wheels can precipitate violation of the constraints and result in degradation in overall system performance (Campion et al., 1996). Hence, the design and control of such vehicles need to first explicitly take into account the maintenance of the kinematic compatibility conditions (before dynamic and/or contact conditions can even be considered).

Most design approaches consider the addition of active or passive articulations between the wheels and chassis to ensure kinematic compatibility. This is pertinent since we consider formation of larger composite wheeled systems by coupling together multiple individual WMRs with an articulated compliant linkage. This allows such systems to accommodate momentary controller errors without transferring any interaction forces between the WMRs. Examples include the CLAPPER and the OMNIMATE (Borenstein et al., 1996), which feature compliant linkages with two passive revolute joints and one passive prismatic joint. However, the biggest limitation of the CLAPPER/OMNIMATE designs comes from the fact that the two WMRs have to stay assembled together because of the compliant linkage.

Fig. 1 CAD models of the (a) individual module (b) composite wheeled system with their corresponding physical prototypes below in (c) and (d) respectively



Hence, we propose the alternate development of a composite wheeled system with a modular formation of the articulated compliant linkage between the wheeled bases. While we will focus the discussion around a 2-module/payload composite system for the rest of the paper, we would like to make some general observations. *First*, our selection of the topology of the individual mobile manipulator modules is guided by the requirement for modularity (in terms of easy attachment/detachment of multiple such modules to a common payload while maintaining at least three d.o.f. within each sub-chain). In this light, we note that a passive planar four-bar mechanism is formed when two such modules attach to a payload—and this articulated linkage introduces more than the minimum (three) required d.o.f. between the bases. However, such excess mobility within the articulated superstructure is eliminated when the more general case of three or more modules is considered. *Second*, we assume that the second link (shown as a “flat support” in Fig. 1(a)) is rigidly attached to the payload. It is worth noting that a variety of other joints may be formed by relaxing this rigid attachment requirement; a discussion of these alternatives, however, is beyond the scope of this paper.

1.2 Research issues

We see that while the articulated compliant linkage resolves the issue of maintenance of compatibility conditions, it introduces a variety of other challenges. First, it creates holonomic (loop closure) constraints that limit the d.o.f. Hence, careful selection of the type and number of joints within the linkage as well as the configuration parameters (link lengths and initial pose) is critical and these aspects are examined elsewhere (Abou-Samah and Krovi, 2002; Tang, 2004). Further, the restriction in d.o.f. due to the holonomic constraints translates into the fact that not all joints need to be actuated. The selection of the location of active and passive joints within the compliant linkage is yet another design choice that plays an important role in determining the payload transport performance (Tang and Krovi, 2004).

The unique contributions of this paper come from the development and evaluation of control schemes for the composite wheeled vehicle that facilitate maintenance of all kinematic (holonomic and nonholonomic) constraints within such systems. Given an arbitrary end-effector trajectory, each individual mobile-manipulator’s bi-level hierarchical controller first generates a *kinematically-feasible desired trajectory* for the WMR base, which is then tracked by a suitable lower-level posture stabilizing controller. While the mechanical articulated structure facilitates accommodation of disturbances within the mobile manipulators, such a controller ensures the maintenance of relative configuration while tracking the desired end-effector trajectory. The composite wheeled vehicle controllers, built up from these

individual mobile-manipulator controllers, now allow for accommodation, detection and correction of relative formation errors and help maintain desired formations. These system-level controllers are also well-suited for online implementation from the viewpoint of both ease of incorporation of local sensor data and computational efficiency.

The rest of the paper is organized as follows: Section 2 provides a brief summary of the pertinent literature. In Section 3, we present the development of the kinematically-compatible controllers for the individual mobile-manipulators that can help maintain a desired configuration while tracking a given end-effector motion trajectory. In Section 4, we derive two variants of system-level cooperative control schemes—leader-follower and decentralized—based on the controllers developed for the individual mobile manipulator. Section 5 describes the hardware and software implementation framework of our system with experimental results presented in Section 6. Section 7 concludes the paper with a discussion.

2 Literature survey

Mobile manipulator systems are typically composed of a WMR platform with one (or more) mounted manipulators (Honzik, 2000; Seraji, 1998; Yamamoto, 1994; Yamamoto and Yun, 1994). While track-, gantry- or manipulator-bases may be modeled and analyzed easily, WMR bases offer special challenges. WMRs cannot be stabilized to a single equilibrium point by a continuous (smooth) time-invariant pure state feedback law, due to the violation of Brockett’s condition (Brockett, 1981). Hence, the motion planning and control of such WMRs requires special treatment (Canudas de Witt et al., 1996; Latombe, 1991; Li and Canny, 1993; Murray and Sastry, 1993). Concomitantly the class of non-holonomic mobile manipulator with such bases requires careful handling.

Further, combining the mobility of the base platform and the mounted manipulator creates redundancy (Seraji, 1998; Yamamoto and Yun, 1994). The determination of the actuator rates for a given end-effector motion of a redundant manipulator is typically an under-constrained problem but essential for motion planning/control of such systems. Most of the redundancy resolution methods available in the literature have a principal underlying theme of optimizing a measure of performance based on kinematics (or in some cases the dynamics) of the system. See Nakamura (1991) for a review of these methods.

Several of these results have been extended and applied to mobile manipulators. Seraji’s (1998) extension of Whitney’s (1969) approach to kinematic redundancy resolution of mobile manipulators hinges on a fully actuated manipulator configuration. This makes it difficult to adapt

this approach to our case, since our mobile manipulator possesses a mixture of active and passive joints. Alternatively, Yamamoto and Yun (1994) decompose the motion of the mobile manipulator into decoupled WMR-base and manipulator subsystems. The WMR is then controlled so as to bring the manipulator to a preferred configuration (using criteria such as the manipulability measure) as the end-effector performs a variety of unknown manipulation tasks. This approach lends itself better to decentralized planning and control, and we develop our controllers in this paper building on this approach.

Our situation is one where the agents physically interact with each other—lesser literature exists but with considerable variety in their proposed approaches. Some approaches emphasize cooperative physical manipulation by teams of relatively simple pushing mobile robots (Donald et al., 1997; Kube and Zhang, 1997; Spletzer et al., 2001; Stilwell and Bay, 1993; Wang et al., 1994). Khatib et al. (1996) used a decentralized control structure for cooperative tasks with mobile manipulation systems, but with holonomic bases and fully actuated manipulators. Others have considered development of optimal motion-planning/control schemes (Desai and Kumar, 1999) and control schemes for nonholonomic cooperating mobile manipulators grasping and transporting payload (Adams et al., 1996), including the effects of flexibility (Tanner et al., 1998) but only from a centralized perspective. Furthermore, in almost all cases, the focus is on a fully actuated manipulator, without any passive or semi-passive joints, which is a dominant feature in our system. Relatively limited literature discusses design/control modifications intended to aid the decentralization of cooperation task, including approaches of selective locking/unlocking of joints (Kosuge et al., 1998) and/or special mechanical designs of the couplings between the multiple manipulators (Humberstone and Smith, 2000).

3 Kinematic control

In this section, we present the development of a bi-level hierarchical control implementation that enforces the kinematic compatibility condition for the individual mobile manipulator. The implementation combines an upper-level design of the kinematically-compatible desired trajectories for the WMRs which are then tracked using a lower-level posture stabilization controller.

3.1 Modeling of the individual mobile manipulators

Figure 2 depicts a differentially-driven WMR with the base of an RRR-manipulator¹ mounted at the midpoint of the

¹R indicates revolute joint. RRR indicates serial linkages connected by three revolute joints.

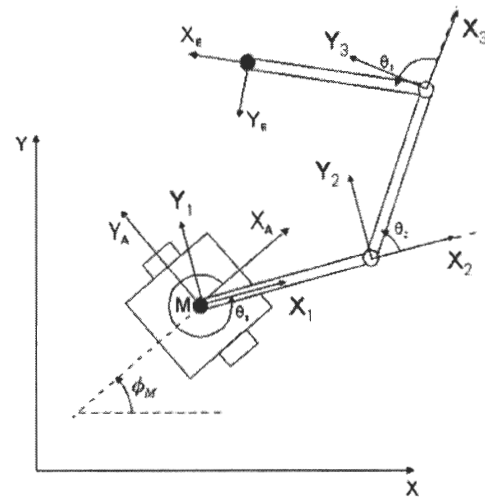


Fig. 2 Schematic diagram of a 3-link mobile manipulator

wheel axle. The frame $\{M\}$ is rigidly attached to the WMR with the X -axis oriented in the direction of the forward travel. Frames $\{1\}$, $\{2\}$ and $\{3\}$ are rigidly attached at the proximal ends of the first, second and third link, respectively. Frame $\{E\}$ is attached at the end-effector of the planar manipulator. The configuration of the manipulator can be parameterized by three relative angles of θ_1 , θ_2 and θ_3 . The lengths of the manipulator links are L_1 , L_2 and L_3 , respectively, ordered from the base. The configuration of the WMR can be described by the position (X_M, Y_M) and the orientation ϕ_M of frame $\{M\}$ with respect to the global frame $\{F\}$. The forward kinematics of the location of frame $\{E\}$ with respect to frame $\{F\}$ can be written as:

$$\begin{bmatrix} X_E \\ Y_E \end{bmatrix} = \begin{bmatrix} X_M \\ Y_M \end{bmatrix} + \begin{bmatrix} \cos \phi_M & -\sin \phi_M \\ \sin \phi_M & \cos \phi_M \end{bmatrix} \times \begin{bmatrix} L_1 \cos \theta_1 + L_2 \cos \theta_{12} + L_3 \cos \theta_{123} \\ L_1 \sin \theta_1 + L_2 \sin \theta_{12} + L_3 \sin \theta_{123} \end{bmatrix}$$

$$\Theta_E = \phi_M + \theta_{123} \tag{1}$$

where $\theta_{12\dots n} = \theta_1 + \theta_2 + \dots + \theta_n$.

3.2 Upper-level desired trajectory creation for kinematic compatibility

In this approach, an arbitrary desired trajectory is specified for the end-effector of each mobile manipulator $\{E\}$. For a given desired manipulator configuration, this allows computation of the corresponding desired trajectory for the reference frame $\{1\}$, fixed rigidly to the first manipulator link. In general, the computed desired trajectories for $\{1\}$ tend to be unsuitable for the frame $\{M\}$ (which is collocated but WMR-fixed) since they may not satisfy the nonholonomic constraints of the WMR. However, we take advantage of the

collocation of the base joint of the manipulator with the midpoint of the wheel axle to then explicitly develop reference trajectories for frame $\{M\}$ that also satisfy the nonholonomic constraints.

As seen in Fig. 2, locating the base of the manipulator at the midpoint of the axle introduces a coupling between the base joint angle θ_1 and WMR orientation ϕ_M :

$$\gamma = \phi_M + \theta_1 \tag{2}$$

Thus Eq. (1) may now be rewritten as:

$$\begin{aligned} \Theta_E &= \gamma + \theta_{23} \\ \begin{bmatrix} X_E \\ Y_E \end{bmatrix} &= \begin{bmatrix} X_M \\ Y_M \end{bmatrix} + \begin{bmatrix} \cos \gamma & -\sin \gamma \\ \sin \gamma & \cos \gamma \end{bmatrix} \\ &\quad \times \begin{bmatrix} L_1 + L_2 \cos \theta_2 + L_3 \cos \theta_{23} \\ L_2 \sin \theta_2 + L_3 \sin \theta_{23} \end{bmatrix} \end{aligned} \tag{3}$$

Note that the vector $[L_1 + L_2 \cos \theta_2 + L_3 \cos \theta_{23}, L_2 \sin \theta_2 + L_3 \sin \theta_{23}]^T$ in the above expression is nothing more than the position vector of the end effector $\{E\}$ with respect to $\{1\}$. Also note that the time-history of the desired² relative manipulator configuration i.e., $\theta_2^d(t), \theta_3^d(t)$, and their time derivatives is known. Hence, given a desired end-effector trajectory $(X_E^d(t), Y_E^d(t), \Theta_E^d(t))$, and a preferred manipulator relative-configuration $(\theta_2^d(t), \theta_3^d(t))$, an expression for the desired trajectory $(X_M^d(t), Y_M^d(t), \gamma^d(t))$ can be obtained as:

$$\begin{aligned} \gamma^d &= \Theta_E^d - \theta_{23}^d \\ \begin{bmatrix} X_M^d \\ Y_M^d \end{bmatrix} &= \begin{bmatrix} X_E^d \\ Y_E^d \end{bmatrix} - \begin{bmatrix} \cos \gamma^d & -\sin \gamma^d \\ \sin \gamma^d & \cos \gamma^d \end{bmatrix} \\ &\quad \times \begin{bmatrix} L_1 + L_2 \cos \theta_2^d + L_3 \cos \theta_{23}^d \\ L_2 \sin \theta_2^d + L_3 \sin \theta_{23}^d \end{bmatrix} \end{aligned} \tag{4}$$

However, at this stage, the calculated $\gamma^d(t)$ cannot be resolved into a desired orientation of the WMR, $\phi_M^d(t)$, and a desired orientation of the first link $\theta_1^d(t)$. Differentiating Eq. (4), we obtain the desired velocity of frame $\{M\}$ as:

$$\begin{aligned} \dot{\gamma}^d &= \dot{\Theta}_E^d - \dot{\theta}_{23}^d \\ \begin{bmatrix} \dot{X}_M^d \\ \dot{Y}_M^d \end{bmatrix} &= \begin{bmatrix} \dot{X}_E^d \\ \dot{Y}_E^d \end{bmatrix} - \begin{bmatrix} -\sin \gamma^d & -\cos \gamma^d \\ \cos \gamma^d & -\sin \gamma^d \end{bmatrix} \end{aligned}$$

² We denote “desired” quantities using superscript d in the rest of the paper.

$$\begin{aligned} &\times \begin{bmatrix} L_1 + L_2 \cos \theta_2^d + L_3 \cos \theta_{23}^d \\ L_2 \sin \theta_2^d + L_3 \sin \theta_{23}^d \end{bmatrix} \dot{\gamma}^d \\ &- \begin{bmatrix} \cos \gamma^d & -\sin \gamma^d \\ \sin \gamma^d & \cos \gamma^d \end{bmatrix} \\ &\times \begin{bmatrix} -L_2 \sin \theta_2^d - L_3 \sin \theta_{23}^d & -L_3 \sin \theta_{23}^d \\ L_2 \cos \theta_2^d + L_3 \cos \theta_{23}^d & L_3 \cos \theta_{23}^d \end{bmatrix} \begin{bmatrix} \dot{\theta}_2^d \\ \dot{\theta}_3^d \end{bmatrix} \end{aligned} \tag{5}$$

We note that since frame $\{M\}$ is rigidly attached to the WMR with its X -axis aligned with its direction of forward travel. This permits us to *uniquely determine* both the desired orientation of frame $\{M\}$, ϕ_M , and the magnitude of the desired forward velocity, v_M^d from Eq. (5) as:

$$\phi_M^d = \tan^{-1} \left(\frac{\dot{Y}_M^d}{\dot{X}_M^d} \right) \tag{6}$$

$$v_M^d = \sqrt{(\dot{X}_M^d)^2 + (\dot{Y}_M^d)^2} \tag{7}$$

Differentiating Eq. (6), we then yield the expression for the angular velocity of frame $\{M\}$, ω_M^d as:

$$\omega_M^d = \left[\frac{\dot{X}_M^d \ddot{Y}_M^d - \dot{Y}_M^d \ddot{X}_M^d}{(\dot{X}_M^d)^2} \right] \cos^2 \phi_M^d \tag{8}$$

Hence, any desired time-trajectory for the end-effector $(X_E^d(t), Y_E^d(t), \Theta_E^d(t))$ can now be transformed into a trajectory $(X_M^d(t), Y_M^d(t), \phi_M^d(t))$ (and the derived forward linear and angular speeds $(v_M^d(t), \omega_M^d(t))$) of a suitable virtual unicycle robot creating the reference trajectory for the WMR. The strategy is well-suited for implementation as an online sensor-based motion planning scheme (using the encoder measurements from the articulations) with good drift-detection and drift-correction performance seen in the experiments. However, it is worth noting that the kinematic compatibility equations above are enforced solely at the velocity/differential level. Hence, care must be taken to initialize the algorithm from an appropriate relative system configuration (see Appendix A for details).

3.3 Lower-level posture stabilizing controller

Samson and Ait-Abderrahim (1991a, 1991b) proposed the use of a “Virtual Robot Algorithm” (VRA) using a continuous time-varying nonlinear feedback for the posture-tracking problem for WMRs. We adopt this technique for controlling the WMR-base of each nonholonomic mobile manipulator to track the desired/planned trajectories discussed in Section 3.2.

A desired/planned trajectory is given as a time-history of the pose of the WMR frame $(X_M^d(t), Y_M^d(t), \phi_M^d(t))$ and its forward translational and angular velocities $(v_M^d(t), \omega_M^d(t))$. As seen in Fig. 3, the VRA assumes that the reference trajectory is generated by suitable selection of a bounded forward velocity, $v_M^r(t) = v_M^d(t)$, and a bounded angular velocity, $\omega_M^r(t) = \omega_M^d(t)$, of a reference unicycle robot³:

$$\begin{bmatrix} \dot{X}_M^r \\ \dot{Y}_M^r \\ \dot{\phi}_M^r \end{bmatrix} = \begin{bmatrix} \cos \phi_M^r & 0 \\ \sin \phi_M^r & 0 \\ 0 & 1 \end{bmatrix} \begin{bmatrix} v_M^r \\ \omega_M^r \end{bmatrix} \tag{9}$$

whose Cartesian velocities may be integrated to update the reference robot pose $\mathbf{q}^r = [X_M^r \ Y_M^r \ \phi_M^r]^T$. For a given pose of the WMR $\mathbf{q} = [X_M \ Y_M \ \phi_M]^T$, the goal is to determine a feedback control law for the actual robot $[\frac{v_M}{\omega_M}] = G(\mathbf{q}, \mathbf{q}^r, v_M^r, \omega_M^r)$ such that $\lim_{t \rightarrow \infty} [\mathbf{q}(t) - \mathbf{q}^r(t)] = 0$. This error $\mathbf{q}(t) - \mathbf{q}^r(t)$ may be expressed in the actual robot's moving frame $\{M\}$ in the form of the auxiliary error function as:

$$\mathbf{e} = \begin{bmatrix} e_1 \\ e_2 \\ e_3 \end{bmatrix} = \begin{bmatrix} \cos \phi_M & \sin \phi_M & 0 \\ -\sin \phi_M & \cos \phi_M & 0 \\ 0 & 0 & 1 \end{bmatrix} \begin{bmatrix} X_M^r - X_M \\ Y_M^r - Y_M \\ \phi_M^r - \phi_M \end{bmatrix} \tag{10}$$

Differentiating Eq. (10) with respect to time yields the open-loop error dynamics:

$$\dot{\mathbf{e}} = \begin{bmatrix} \dot{e}_1 \\ \dot{e}_2 \\ \dot{e}_3 \end{bmatrix} = \begin{bmatrix} 0 & \omega_M & 0 \\ -\omega_M & 0 & 0 \\ 0 & 0 & 0 \end{bmatrix} \begin{bmatrix} e_1 \\ e_2 \\ e_3 \end{bmatrix} + \begin{bmatrix} v_M^r \cos e_3 - v_M \\ v_M^r \sin e_3 \\ \omega_M^r - \omega_M \end{bmatrix} \tag{11}$$

Under a suitable change of inputs (shown below):

$$\begin{bmatrix} u_1 \\ u_2 \end{bmatrix} = \begin{bmatrix} v_M^r \cos e_3 - v_M \\ \omega_M^r - \omega_M \end{bmatrix} \tag{12}$$

the closed-loop nonlinear feedback controller for the system in Eq. (11) may be written as:

$$\begin{bmatrix} u_1 \\ u_2 \end{bmatrix} = \begin{bmatrix} -k_1 (v_M^r, \omega_M^r) e_1 \\ -k_4 v_M^r \frac{\sin e_3}{e_3} e_2 - k_3 (v_M^r, \omega_M^r) e_3 \end{bmatrix}$$

³ Reference robot variables are denoted using superscript *r* and actual robot variables without any superscript for the rest of the paper.

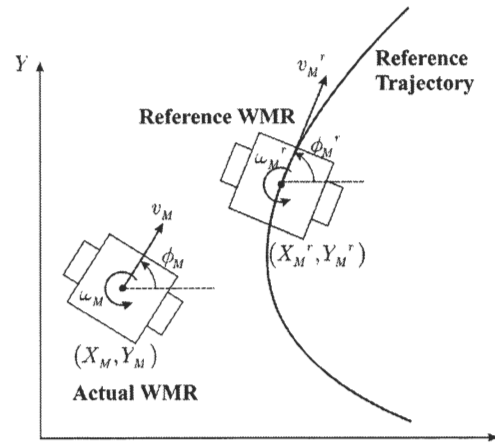


Fig. 3 Notation used for the Virtual Robot Algorithm wherein the actual WMR tracks a reference WMR (with unicycle kinematics) traveling along the given trajectory

$$\begin{aligned} k_1 (v_M^r, \omega_M^r) &= k_3 (v_M^r, \omega_M^r) \\ &= 2\zeta \sqrt{(\omega_M^r)^2 + b (v_M^r)^2}, k_4 = b \\ &b > 0, \zeta > 0 \end{aligned} \tag{13}$$

However, this original nonlinear feedback requires that the $v_M^r(t)$ and $\omega_M^r(t)$ never become simultaneously zero for guaranteeing convergence. Hence, in the subsequent extension, Samson and Ait-Abderrahim (1991b) alter the reference robot velocities as:

$$\begin{aligned} v_M^r &= v_M^d - k_4 \text{sgn}(X_M - X_M^r) \sqrt{(X_M - X_M^r)^2 + (Y_M - Y_M^r)^2} \\ &\quad + (e_1^2 + e_2^2 + e_3^2) \sin t \\ \omega_M^r &= \omega_M^d \end{aligned} \tag{14}$$

This modification prevents the reference robot velocities from becoming zero while a pose-error exists—which then allows a direct use of the original non-linear feedback law for the posture-stabilization problem. An interested reader is referred to Samson and Ait-Abderrahim (1991a, 1991b) or Chapter 7 in Canudas de Witt et al. (1996) for the detailed discussion.

4 Kinematic collaboration of two mobile manipulators

We now examine two variants of system-level cooperative control schemes—leader-follower and decentralized control—that can be created based on the individual mobile-manipulator control scheme.

4.1 Leader-follower approach

The first method of modeling such a system considers the midpoint of the mobile base (MP B) of the mobile-manipulator B to be rigidly attached to the end-effector of mobile manipulator A, as depicted in Fig. 4. Figure 4(b) depicts how the end-effector frame $\{E\}$ of MP A is rigidly attached to the frame $\{B\}$ at MP B (separated by a constant rotation angle β).

$$\Theta_E^d = \Theta_B^d + \beta$$

$$\begin{bmatrix} X_E^d \\ Y_E^d \end{bmatrix} = \begin{bmatrix} \cos \beta & -\sin \beta \\ \sin \beta & \cos \beta \end{bmatrix} \begin{bmatrix} X_B^d \\ Y_B^d \end{bmatrix} \tag{15}$$

MP B now takes on the role of the leader and can be controlled to follow any trajectory that is feasible for a WMR. Hence, given a trajectory of the leader MP B ($X_B^d(t), Y_B^d(t), \Theta_B^d(t)$), and the preferred manipulator configuration of ($\theta_2^d(t), \theta_3^d(t)$), Eq. (5) can be rewritten as:

$$\dot{\gamma}^d = \dot{\Theta}_B^d - \dot{\theta}_2^d - \dot{\theta}_3^d$$

$$\begin{bmatrix} \dot{X}_A^d \\ \dot{Y}_A^d \end{bmatrix} = \begin{bmatrix} \cos \beta & -\sin \beta \\ \sin \beta & \cos \beta \end{bmatrix} \begin{bmatrix} \dot{X}_B^d \\ \dot{Y}_B^d \end{bmatrix}$$

$$- \begin{bmatrix} -\sin \gamma^d & -\cos \gamma^d \\ \cos \gamma^d & -\sin \gamma^d \end{bmatrix}$$

$$\times \begin{bmatrix} L_1 + L_2 \cos \theta_2^d + L_3 \cos \theta_{23}^d \\ L_2 \sin \theta_2^d + L_3 \sin \theta_{23}^d \end{bmatrix} \dot{\gamma}^d$$

$$- \begin{bmatrix} \cos \gamma^d & -\sin \gamma^d \\ \sin \gamma^d & \cos \gamma^d \end{bmatrix}$$

$$\times \begin{bmatrix} -L_2 \sin \theta_2^d - L_3 \sin \theta_{23}^d & -L_3 \sin \theta_{23}^d \\ L_2 \cos \theta_2^d + L_3 \cos \theta_{23}^d & L_3 \cos \theta_{23}^d \end{bmatrix} \begin{bmatrix} \dot{\theta}_2^d \\ \dot{\theta}_3^d \end{bmatrix}$$

and correspondingly Eqs. (6)–(8) as:

$$\phi_A^d = \tan^{-1} \left(\frac{\dot{Y}_A^d}{\dot{X}_A^d} \right), \quad v_A^d = \sqrt{(\dot{X}_A^d)^2 + (\dot{Y}_A^d)^2}$$

$$\omega_A^d = \left[\frac{\dot{X}_A^d \ddot{Y}_A^d - \dot{Y}_A^d \ddot{X}_A^d}{(\dot{X}_A^d)^2} \right] \cos^2 \phi_A^d \tag{17}$$

Thus, the trajectory of the virtual (reference) robot for the follower MP A ($X_A^d(t), Y_A^d(t), \phi_A^d(t)$), and the derived velocities ($v_A^d(t), \omega_A^d(t)$) can now be determined. This forms the leader-follower scheme used for the control of the collaborative system carrying a common payload.

4.2 Decentralized approach

The second approach considers the frame attached to a point of interest on the common payload as the end-effector frame of both the flanking mobile manipulator systems, as depicted in Fig. 5. Thus, a desired trajectory specified for this payload frame can then provide the desired reference trajectories for the two mobile platforms using the similar framework developed in the previous section by taking ${}^k L_3 = 0$ and ${}^k \theta_3(t) = 0$, where $k = A, B$. This permits Eq. (5) to be rewritten as:

$${}^k \dot{\gamma}^d = \dot{\Theta}_E^d - {}^k \dot{\theta}_2^d$$

$$\begin{bmatrix} {}^k \dot{X}_M^d \\ {}^k \dot{Y}_M^d \end{bmatrix} = \begin{bmatrix} {}^k \dot{X}_E^d \\ {}^k \dot{Y}_E^d \end{bmatrix}$$

$$- \begin{bmatrix} -\sin {}^k \gamma^d & -\cos {}^k \gamma^d \\ \cos {}^k \gamma^d & -\sin {}^k \gamma^d \end{bmatrix}$$

$$\times \begin{bmatrix} {}^k L_1 + {}^k L_2 \cos {}^k \theta_2^d \\ {}^k L_2 \sin {}^k \theta_2^d \end{bmatrix} {}^k \dot{\gamma}^d$$

$$- \begin{bmatrix} \cos {}^k \gamma^d & -\sin {}^k \gamma^d \\ \sin {}^k \gamma^d & \cos {}^k \gamma^d \end{bmatrix} \begin{bmatrix} -{}^k L_2 \sin {}^k \theta_2^d \\ {}^k L_2 \cos {}^k \theta_2^d \end{bmatrix} {}^k \dot{\theta}_2^d \tag{18}$$

and correspondingly Eq. (6)–(8) as:

$${}^k \phi_M^d = \tan^{-1} \left(\frac{{}^k \dot{Y}_M^d}{{}^k \dot{X}_M^d} \right), \quad {}^k v_M^d = \sqrt{({}^k \dot{X}_M^d)^2 + ({}^k \dot{Y}_M^d)^2}$$

$${}^k \omega_M^d = \left[\frac{{}^k \dot{X}_M^d {}^k \ddot{Y}_M^d - {}^k \dot{Y}_M^d {}^k \ddot{X}_M^d}{({}^k \dot{X}_M^d)^2} \right] \cos^2 ({}^k \phi_M^d) \tag{19}$$

Each two-link mobile manipulator now controls its configuration with reference to this common end-effector frame mounted on the payload. However, the locations of the attachments of the physical manipulators with respect to the payload reference frame must be known a priori.

5 Implementation framework

We examine the design and development of a two-stage implementation framework, shown in Fig. 6, that emphasizes both virtual prototyping (VP) based refinement and hardware-in-the-loop (HIL) experimentation.

5.1 Virtual prototyping based refinement

In the first stage, we employ *virtual prototyping* (VP) tools to rapidly create, evaluate and refine parametric models of

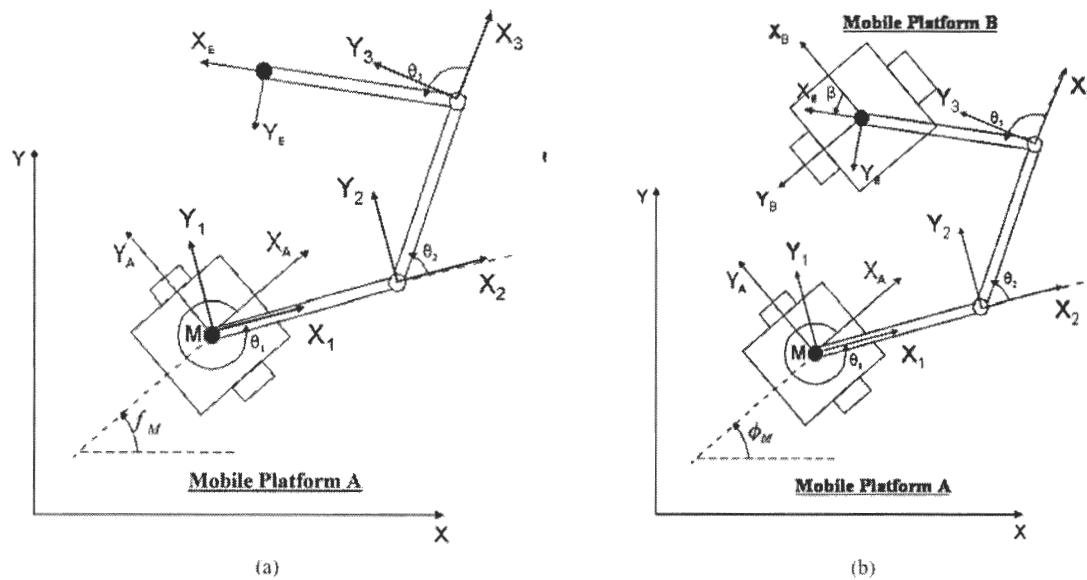


Fig. 4 Schematic diagrams of the leader-follower scheme: (a) the 3-link mobile manipulator under analysis, and (b) the two-module composite system

the overall system and test various algorithms in simulation within a virtual environment. 3D solid models of the mobile platforms and the manipulators of interest are created in a CAD package,⁴ and exported with their corresponding geometric and material properties into a dynamic simulation environment.⁵ Figure 7(a) shows an example of the application of such framework for simulating the motion of a mobile platform controlled by an algorithm implemented in Simulink.⁶ However, it is important to note that the utility of such virtual testing is limited by: (a) the ability to correctly model and simulate the various phenomena within the virtual environment; (b) the fidelity of the available simulation tools; and (c) ultimately, the ability of the designer to correctly model the desired system and suitably interpret the results.

5.2 Hardware-in-the-loop experimentation

We employ a *hardware-in-the-loop* (HIL) methodology for rapid experimental verification of the real-time controllers on the electromechanical mobile manipulator prototypes. Each individual WMR is constructed using two powered wheels and two unactuated casters. Conventional disc-type rear wheels, powered by gear-motors, are chosen because of robust physical construction and ease of operation in the presence of terrain irregularities. Passive ball casters are preferred over wheel casters to simplify the constraints on

maneuverability introduced by the casters. The mounted manipulator arm has two passive revolute joints with axes of rotation parallel to each other and perpendicular to the base of the mobile platform. The first joint is placed appropriately at the geometric center on top frame of the platform. The location of the second joint can be adjusted to any position along the slotted first link. The second link itself is reduced to a flat plate supported by the second joint. Each joint is instrumented with optical encoder that can measure the joint rotations. The completely assembled two-link mobile manipulator is shown in Fig. 1(c).

The second mobile manipulator (see left module of Fig. 1(b) and (d)) employs the same overall design but possesses a motor at the base joint of the mounted two-link arm. The motor may be used to control the joint motion along a predetermined trajectory (which can include braking/holding the joint at a predetermined position). When the motor is switched off the joint now reverts to a passive joint (with much greater damping). The motor is included for permitting future force-redistribution studies. In this paper, however, the motor is used solely to lock the joint prevent self-motions of the articulated linkage for certain pathological cases (Bhatt et al., 2005; Tang and Krovi, 2004).

A PC/104 system, equipped with an xPC Target⁷ Real-Time Operating System (RTOS) serves as the embedded controller. PWM-output motor driver cards are used to drive the gearmotors; and encoder cards monitor the encoders instrumenting the various articulated arms. This embedded controller communicates with a designated host computer using TCP/IP for program download and data logging.

⁴ SolidWorksTM was the CAD package used for this work.

⁵ MSC Visual NastranTM was the dynamic simulation environment used for this work.

⁶ Simulink is the registered trademark of Mathworks.

⁷ xPC Target is a product of Mathworks.

Fig. 5 Decentralized control scheme implementation permits the (a) composite system; to be treated as (b) two independent 2-link mobile manipulators

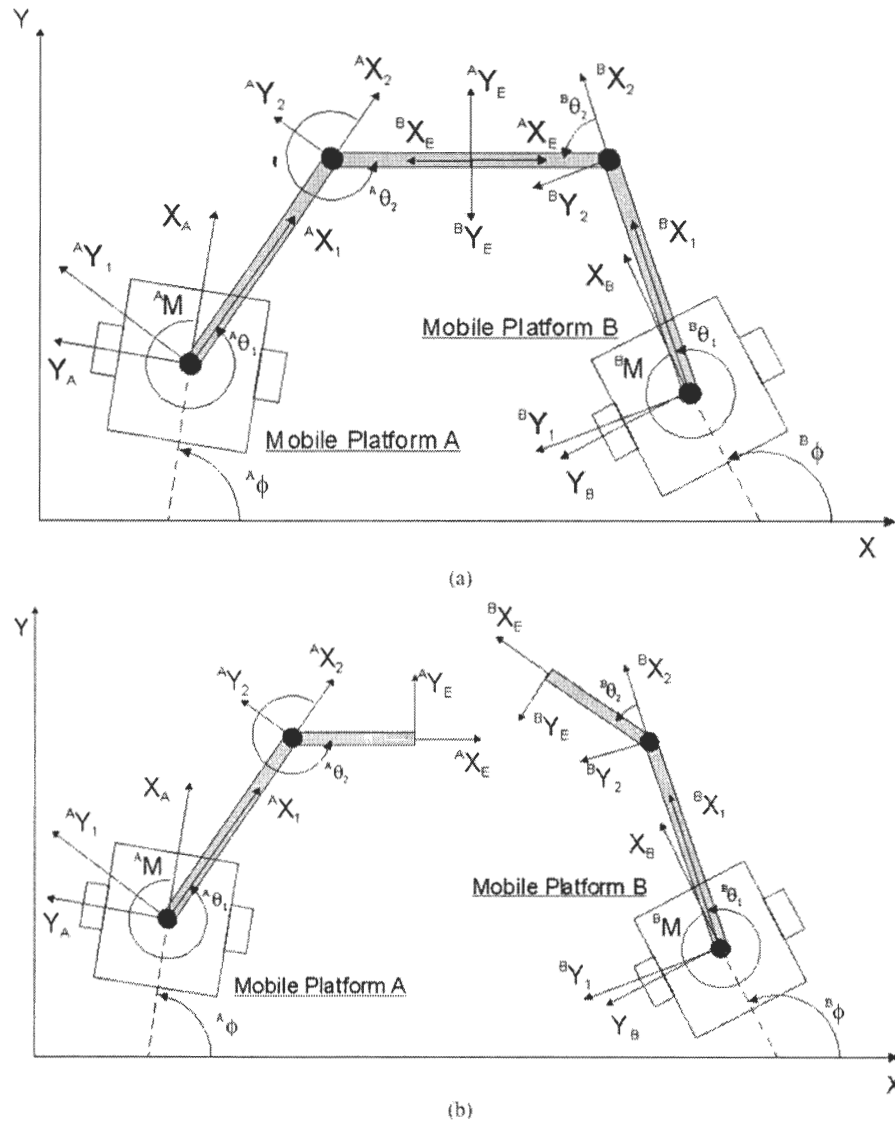
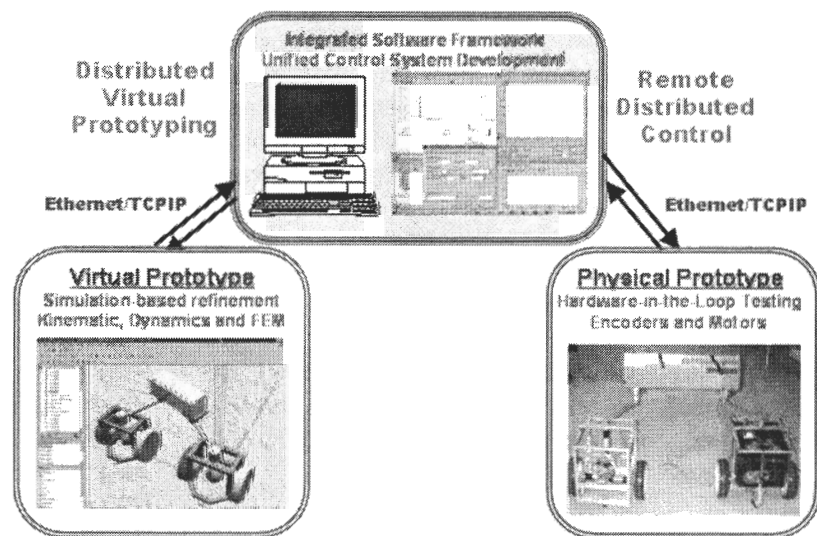


Fig. 6 Paradigm for rapid development and testing of the control scheme on virtual and physical prototypes



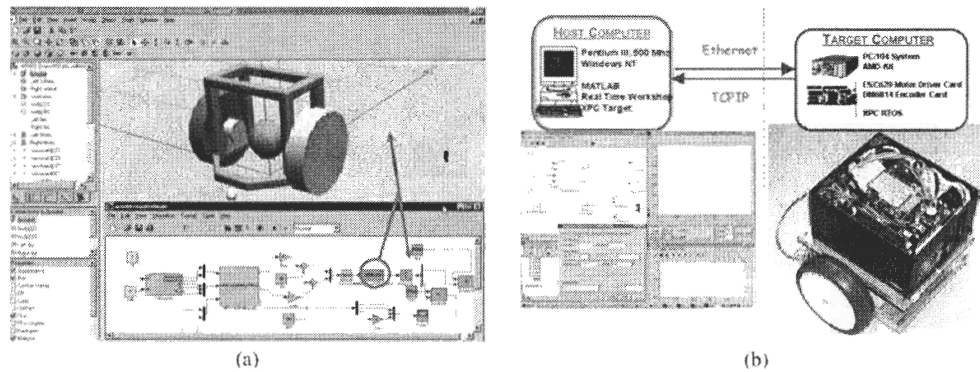


Fig. 7 A single WMR base undergoing testing within the (a) virtual prototyping framework; and (b) hardware-in-the-loop (HIL) testing framework

The host computer with MATLAB/Simulink/Real Time Workshop⁸ provides a convenient graphical user interface environment for system-level software development using a block-diagrammatic language. The compiled executable is downloaded over the network and executes in real-time on the embedded controller while accessing locally installed hardware components.

In particular, the ability to selectively test components/systems at various levels (e.g. individual motors, individual WMRs or entire systems) without wearing out components during design iterations was very useful. Figure 7(b) illustrates the implementation of such a system on one of the WMRs. Numerous calibration, simulation and experimental studies carried out with this framework, at the individual-level and system-level, are reported in Abou-Samah (2001).

6 Experimental results

For the subsequent experiments,⁹ we prescribe the initial configuration of the two-module composite system, as shown in Fig. 8. Specifically, we position the two WMRs such that MP A is located at a relative position of $x = 0.00\text{m}$ (0 in.), $y = 0.61\text{m}$ (24 in.) and with a relative orientation difference of $\delta = 0.00^\circ$ with respect to MP B. For fixed link-lengths this inherently specifies the values of the various configuration angles as shown in Table 1.

6.1 Leader-follower approach

A straight line trajectory at a velocity of 0.0254 m/s is prescribed for the leader, MP B. Given a desired configuration of the manipulator arm, the algorithm described in Section 4.1

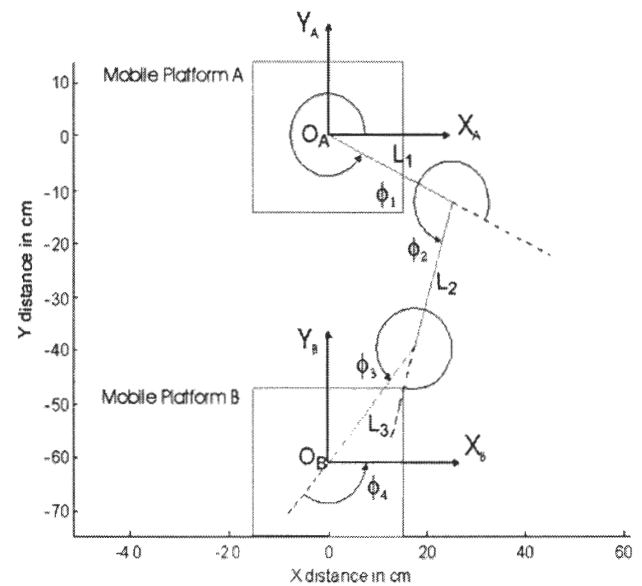


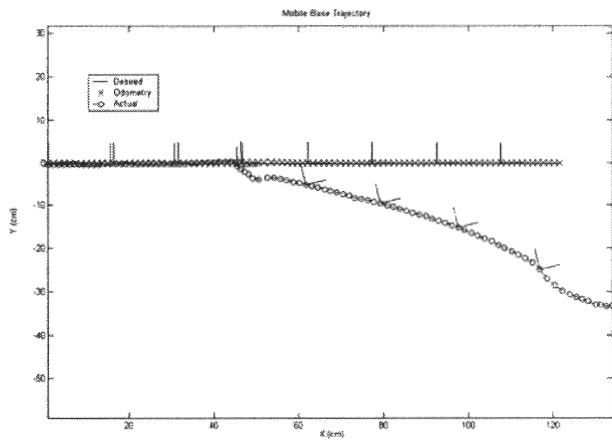
Fig. 8 Initial configuration of the two-module composite wheeled system

is used to obtain a desired trajectory for MP A. A large disruption is intentionally introduced by causing one of the wheels of MP A to run over a bump, to evaluate the effectiveness of the disturbance accommodation, detection and compensation. The results are examined in two case scenarios – *Case A: MP A employs odometric estimation for localization* as seen in Fig. 9, and *Case B: MP A employs sensed articulations for localization* as seen in Fig. 10. In each of these figures, (a) presents the overall (X_M, Y_M) -trajectory of $\{M\}$ of MPA with respect to the end-effector frame $\{E\}$ (that is rigidly attached to the $\{M\}$ of MPB) while (b), (c) and (d) present the relative orientation difference, X -difference and Y -difference as functions of time. Further in both sets of figures, the ‘Desired’ (— line) is the desired trajectory typically computed offline; and ‘Actual’ (–o– line) is the actual trajectory followed by the system, as determined by post-processing the measurements of the instrumented articulations. However, in

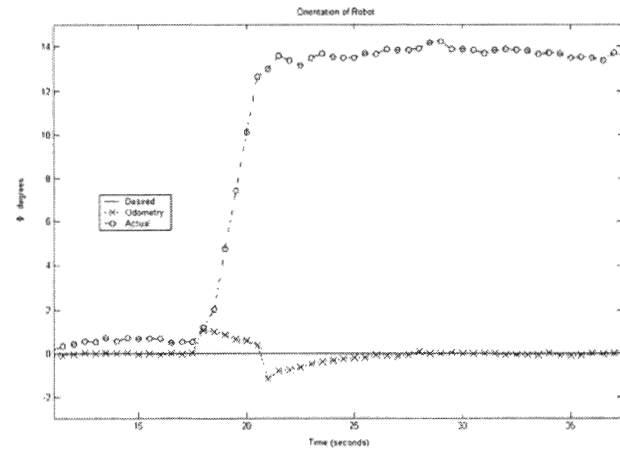
⁸ MATLAB is a registered trademark of Mathworks.
⁹ Videos of experimental evaluation are available at <http://mechatronics.eng.buffalo.edu/research/mobilemanipulator>.

Table 1 Parameters for the initial configuration of the two-module composite wheeled system (see Fig. 8 for details)

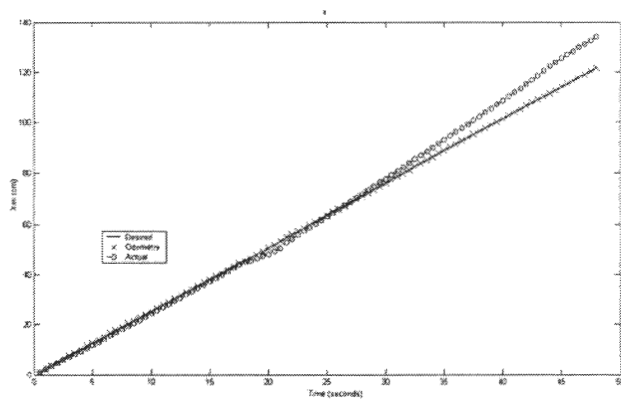
Link lengths of the articulation	L_1	0.28 m (11 in)
	L_2	0.28 m (11 in)
	L_3	0.28 m (11 in)
Relative angles of the configuration of the articulation	ϕ_1	333.98°
	ϕ_2	280.07°
	ϕ_3	337.36°
	ϕ_4	128.59°
Offset between the wheeled mobile bases	δ	0.00°
	$(O_B O_A)_X$	0.00 m (0 in)
	$(O_B O_A)_Y$	0.61 m (24 in)



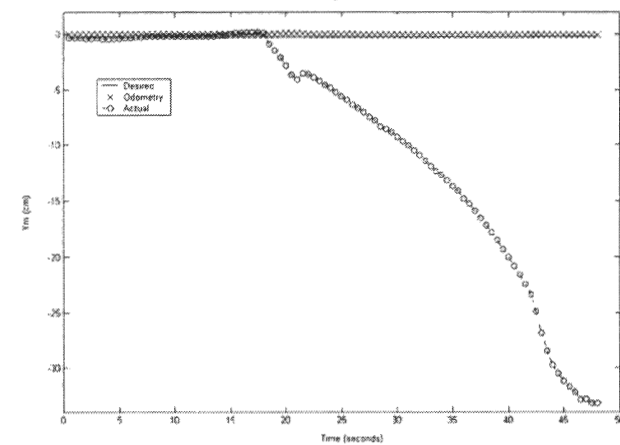
(a)



(b)



(c)



(d)

Fig. 9 Case A: Odometric Estimation of Frame M, used in the control of MP A following MPB in a leader-follower approach, is unable to detect non-systematic errors such as wheel-slip. (a) XY trajectory

of Frame M; (b) Orientation versus Time; (c) X position of Frame M versus Time; and (d) Y position of Frame M versus Time

Fig. 9, the (–x– line) represents the odometric estimate while in Fig. 10 it stands for the articulation based estimate (which therefore coincides with the ‘Actual’ (–o– line) trajectory).

In Case A, the introduction of the disruption causes a drift in the relative configuration of the system which remains undetected by the odometric estimation. Further, as seen in

Fig. 9, this drift has a tendency to grow if left uncorrected. However, as seen in Fig. 10, the system can use the articulation-based estimation (Case B) to not only detect disturbances to the relative configuration but also to successfully restore the original system configuration.

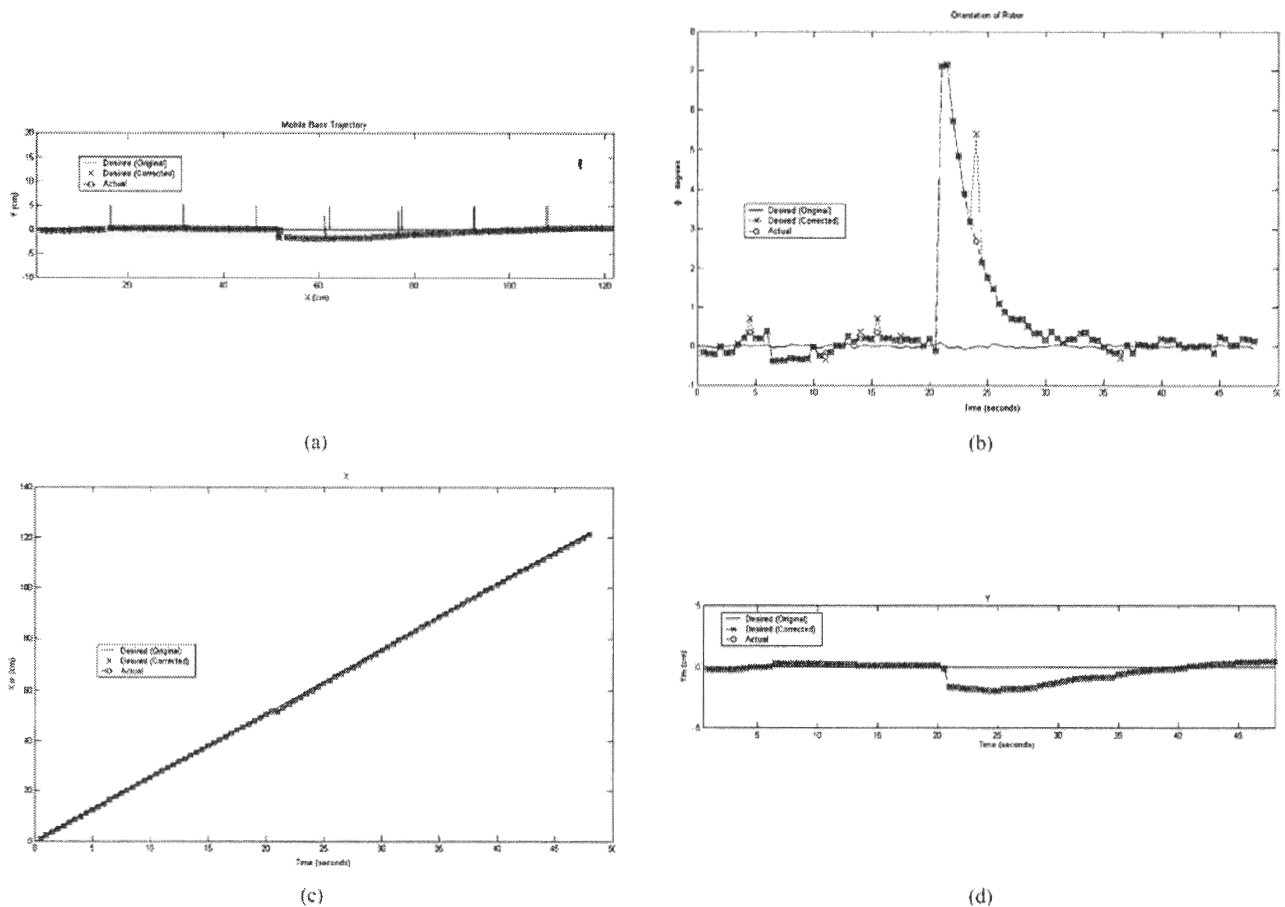


Fig. 10 Case B: Articulation based Estimation of Frame M, used for control of MPA with respect to MP B in a leader-follower approach is able to detect and correct non-systematic errors such as

wheel-slip. (a) XY trajectory of Frame M; (b) Orientation versus Time; (c) X position of Frame M versus time; and (d) Y position of Frame M versus time

6.2 Decentralized control approach

In this decentralized control scenario, a straight line trajectory with a velocity of 0.0254 m/s is presented for the payload frame. As in the leader-follower scenario, a large disruption is introduced by causing one of the wheels of MP A to run over a bump. The algorithm is tested using two further case scenarios—*Case C: Both mobile platforms employ odometric estimation for localization* as shown in Fig. 11, and *Case D: Both mobile platforms employ sensed articulations for localization* as shown in Fig. 12.

In each of these figures, subplots (a) and (b) presents the overall (X_M , Y_M) trajectories of frames $\{M\}$ of MP A and MP B respectively with respect to their initial poses. Subplots (c), (d) and (e) present the relative orientation difference, X-difference and Y-difference of frames $\{M\}$ of MP A and MP B respectively as functions of time. Further in both sets of figures, the ‘Desired’ (— line) is the desired trajectory typically computed offline; and ‘Actual’ (—o— line) is the actual trajectory followed by the system, as determined

by post-processing the measurements of the instrumented articulations. However, in Fig. 11, the (—x— line) represents the odometric estimate while in Fig. 12 it stands for the articulation based estimate.

In Case C, *both mobile platforms use the odometric estimation for localization*—hence as expected, Fig. 11 reflects the fact that the system is unable to detect or correct for changes in the relative system configuration. However the data obtained from the articulations accurately captures the existence of errors between the frames of reference of MP B and MP A. Thus, using the articulation-based estimation of relative configuration for control as in Case D allows the detection of disturbances and successful restoration of the original system configuration as shown in Fig. 12. Note, however, while the relative system configuration is maintained, errors relative to a global reference frame cannot be detected if both WMRs undergo *identical simultaneous disturbances*. Detection of such absolute errors would require an external reference and is beyond the scope of the existing framework.

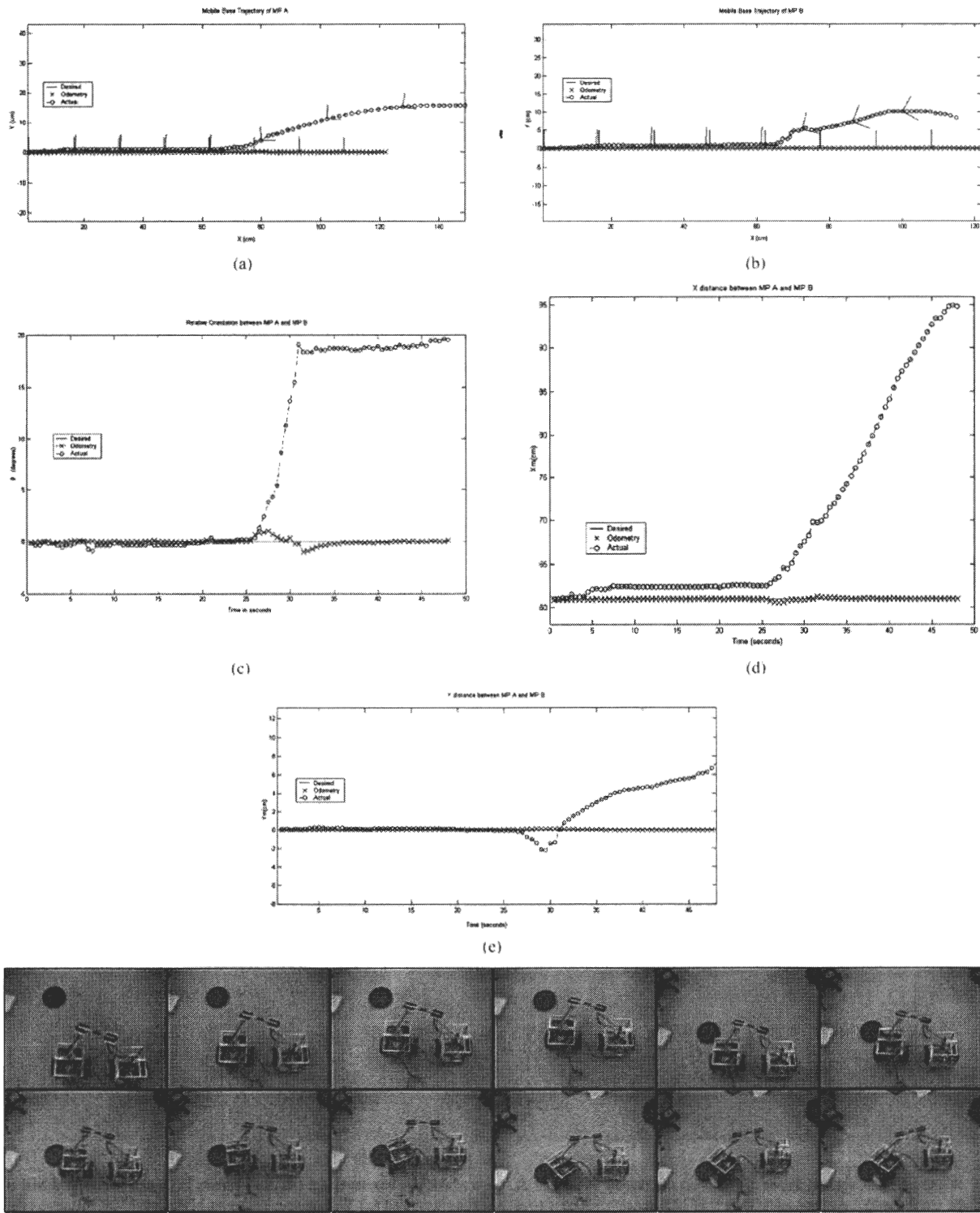


Fig. 11 Case C: Odometric estimation of frames M of MP A and MP B, used in the control of MP A with respect to MP B in the decentralized approach, is again unable to detect non-systematic errors such as wheel-slip. (a) XY trajectory of frame M of MP A; (b) XY trajectory of frame M of MP B; (c) Relative orientation, between MP A and MP B,

versus time; (d) X distance, between MP A and MP B, versus time; and (e) Y distance, between MP A and MP B, versus time. (f) Sequential photographs of the corresponding composite system motion (as time progresses from left to right along each row)

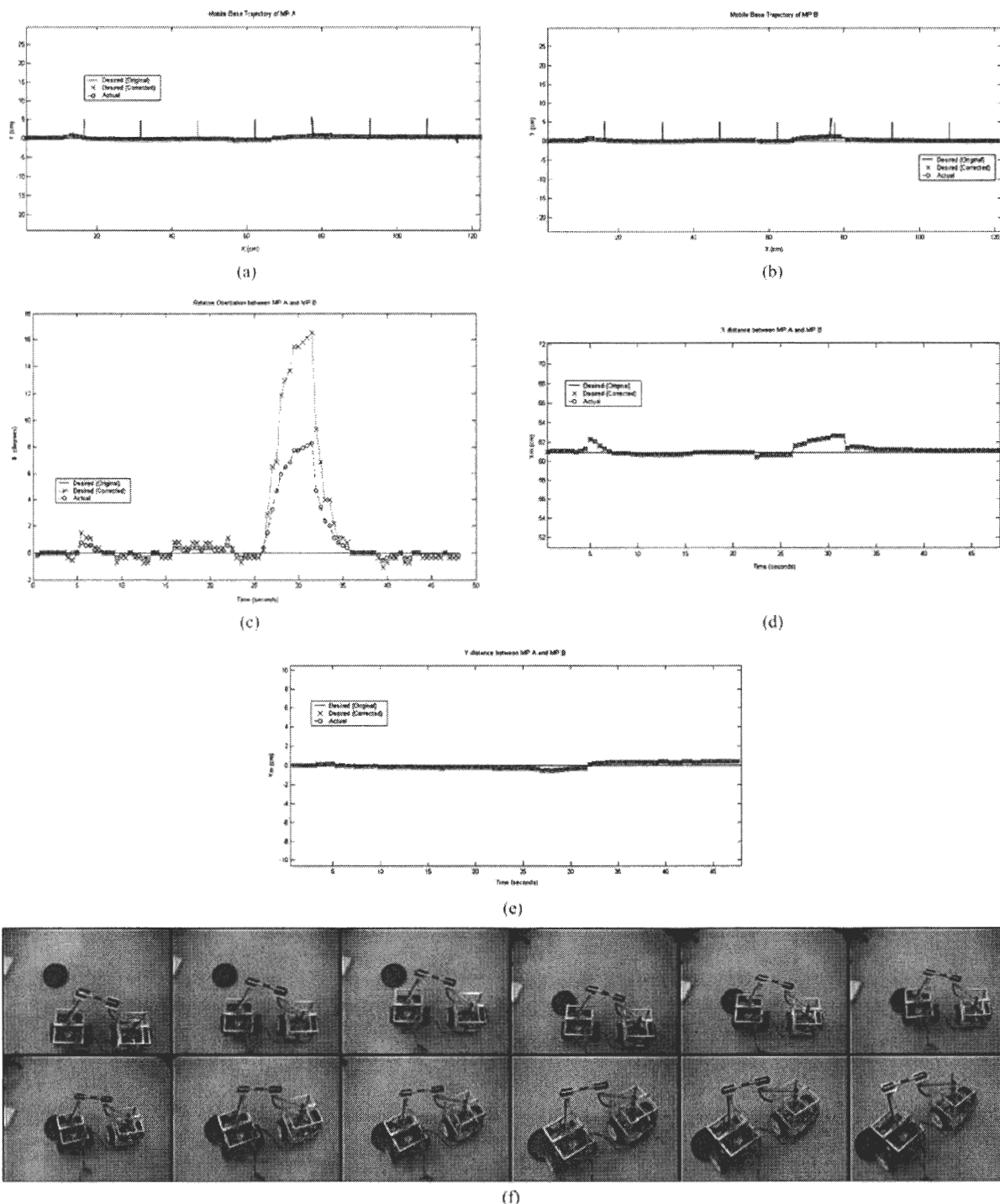


Fig. 12 Case D: Articulation based estimation of frames M of MP A and MP B, used for the control of MP A and MP B with respect to a payload-fixed frame is able to detect and correct non-systematic errors such as wheel-slip. (a) XY trajectory of frame M of MP A; (b) XY trajectory of frame M of MP B; (c) Relative orientation, between MP A

and MP B, versus time; (d) X distance, between MP A and MP B, versus time; and (e) Y distance, between MP A and MP B, versus time. (f) Sequential photographs of the corresponding composite system motion (as time progresses from left to right along each row)

7 Conclusion

In this paper, we examined the design, development and validation of a kinematically compatible framework for co-

operative transport of a common payload by a team of non-holonomic mobile manipulators. Each individual mobile manipulator module consists of a differentially driven wheeled WMR retrofitted with a passive two revolute jointed planar

manipulator arm. A composite multi degree-of-freedom vehicle system could then be modularly created by attaching a common payload on the end-effector of two or more such modules.

The composite system allowed payload trajectory tracking errors, arising from subsystem controller errors or environmental disturbances, to be readily accommodated within the compliance offered by the articulated linkage. The individual mobile manipulators compensated by modifying their WMR bases’ motion plans to ensure prioritized satisfaction of the nonholonomic constraints. The stabilizing controllers of the WMR bases could then track the recomputed “desired motion plans” to help restore the system-configuration. This scheme not only explicitly ensured maintenance of the kinematic compatibility constraints within the system but is also well suited for an online sensor-based motion planning implementation.

This algorithm was then adapted to create two control schemes for *the overall composite system*— the leader follower approach and the decentralized approach. We evaluated both approaches within an implementation framework that emphasized both, virtual prototyping and hardware-in-the-loop using the case-study of a two module composite system. Experimental results verified the ability of the composite system with sensed articulations to not only accommodate instantaneous disturbances due to terrain irregularities but also to detect and correct drift in the relative system configuration. The overall framework readily facilitates generalization to treat larger systems with many more mobile manipulator modules.

Appendix A

The kinematic constraint equations shown in Eq. (3) may be written in the general form as:

$$C(\mathbf{q}, t) = \begin{bmatrix} \Theta_E - \gamma - \theta_2 - \theta_3 \\ \begin{bmatrix} X_E \\ Y_E \end{bmatrix} - \begin{bmatrix} X_M \\ Y_M \end{bmatrix} - \begin{bmatrix} \cos \gamma & -\sin \gamma \\ \sin \gamma & \cos \gamma \end{bmatrix} \begin{bmatrix} L_1 + L_2 \cos \theta_2 + L_3 \cos \theta_{23} \\ L_2 \sin \theta_2 + L_3 \sin \theta_{23} \end{bmatrix} \end{bmatrix} = \mathbf{0} \tag{20}$$

Then the velocity constraint equation can be written as:

$$\dot{C}(\mathbf{q}, t) = \mathbf{0} \tag{21}$$

The general solution to this differential equation is:

$$C(\mathbf{q}, t) = C_0 = C(\mathbf{q}_0, 0) \tag{22}$$

By appropriate selection of the initial conditions within the experimental setup, one can create the condition $C_0 = C(\mathbf{q}_0, 0) = \mathbf{0}$, *i.e.*, exactly satisfying the constraint at the initial time, which then permits the constraint to be satisfied for all time. However, one could also enhance this process by adding another term to the right-hand-side of Eq. (21) as:

$$\dot{C}(\mathbf{q}, t) = -\Phi C(\mathbf{q}, t) \tag{23}$$

where Φ is a positive-definite constant matrix. This results in a first order stable system:

$$\dot{C}(\mathbf{q}, t) + \Phi C(\mathbf{q}, t) = \mathbf{0} \tag{24}$$

whose solution for any arbitrary initial configuration is:

$$C(\mathbf{q}, t) = \exp(-\Phi t)C(\mathbf{q}, 0) \tag{25}$$

In such systems, there is no longer a requirement to enforce $C_0 = C(\mathbf{q}_0, 0) = \mathbf{0}$ since the solution exponentially stabilizes to $C(\mathbf{q}_0, 0) = \mathbf{0}$ regardless of the initial conditions. This feature could potentially be easily added to transform Eq. (5) to further improve overall performance, but was not required.

Acknowledgment We gratefully acknowledge the support of the Canadian Natural Sciences and Engineering Research Council (NSERC), Fonds pour la formation de chercheurs et l’aide la recherche (Fonds FCAR), the McGill Petro-Canada Young Innovator Award, and National Science Foundation CAREER Award (IIS-0347653).

References

Abou-Samah, M. 2001. A kinematically compatible framework for collaboration of multiple non-holonomic wheeled mobile robots. M. Eng. Thesis, McGill University, Montreal, Canada.
 Abou-Samah, M. and Krovi, V. 2002. Optimal configuration selection for a cooperating system of mobile manipulators. In *Proceedings*

- of the 2002 ASME Design Engineering Technical Conferences, DETC2002/MECH-34358, Montreal, QC, Canada.
- Adams, J., Bajcsy, R., Kosecka, J., Kumar, V., Mandelbaum, R., Mintz, M., Paul, R., Wang, C.-C., Yamamoto, Y., and Yun, X. 1996. Cooperative material handling by human and robotic agents: Module development and system synthesis. *Expert Systems with Applications*, 11(2):89–97.
- Bhatt, R.M., Tang, C.P., Abou-Samah, M., and Krovi, V. 2005. A screw-theoretic analysis framework for payload manipulation by mobile manipulator collectives. In *Proceedings of the 2005 ASME International Mechanical Engineering Congress & Exposition, IMECE2005-81525*, Orlando, Florida, USA.
- Borenstein, J., Everett, B., and Feng, L. 1996. *Navigating Mobile Robots: Systems and Techniques*. A. K. Peters, Ltd., Wellesley, MA.
- Brockett, R.W. 1981. Control theory and singular riemannian geometry. In P.J. Hilton and G.S. Young (eds), *New Directions in Applied Mathematics*, Springer-Verlag, New York, pp. 11–27.
- Campion, G., Bastin, G., and D'Andrea-Novel, B. 1996. Structural properties and classification of kinematic and dynamic models of wheeled mobile robots. *IEEE Transactions on Robotics and Automation*, 12(1):47–62.
- Canudas de Witt, C., Siciliano, B., and Bastin, G. 1996. *Theory of Robot Control*. Springer-Verlag, Berlin.
- Desai, J. and Kumar, V. 1999. Motion planning for cooperating mobile manipulators. *Journal of Robotic Systems*, 16(10):557–579.
- Donald, B.R., Jennings, J., and Rus, D. 1997. Information invariants for distributed manipulation. *The International Journal of Robotics Research*, 16(5):673–702.
- Honzik, B. 2000. Simulation of the kinematically redundant mobile manipulator. In *Proceedings of the 8th MATLAB Conference 2000*, Prague, Czech Republic, pp. 91–95.
- Humberstone, C.K. and Smith, K.B. 2000. Object transport using multiple mobile robots with non-compliant endeffectors. In *Distributed Autonomous Robotics Systems 4*. Springer-Verlag, Tokyo, Tokyo, pp. 417–426.
- Juberts, M. 2001. Intelligent control of mobility systems. Needs. ISD Division, Manufacturing Engineering Laboratory, National Institute of Standards and Technology.
- Khatib, O., Yokoi, K., Chang, K., Ruspini, D., Holmberg, R., and Casal, A. 1996. Vehicle/arm coordination and multiple mobile manipulator decentralized cooperation. In *Proceedings of the 1996 IEEE/RSJ International Conference on Intelligent Robots and Systems*, Osaka, Japan, pp. 546–553.
- Kosuge, K., Osumi, T., Sato, M., Chiba, K., and Takeo, K. 1998. Transportation of a single object by two decentralized-controlled nonholonomic mobile robots. In *1998 IEEE International Conference on Robotics and Automation*, Leuven, Belgium, pp. 2989–2994.
- Kube, C.R. and Zhang, H. 1997. Task modelling in collective robotics. *Autonomous Robots*, Kluwer Academic Publishers, 4(1):53–72.
- Latombe, J.-C. 1991. *Robot Motion Planning*. Kluwer Academic Publishers, Boston, MA.
- Li, Z. and Canny, J.F. 1993. *Nonholonomic Motion Planning*. Kluwer Academic Publishers, Boston, MA.
- Murray, R.M. and Sastry, S.S. 1993. Nonholonomic motion planning: Steering using sinusoids. *IEEE Transactions on Automatic Control*, 38(5):700–716.
- Nakamura, Y. 1991. *Advanced Robotics: Redundancy and Optimization*. Addison-Wesley Publishing Company, Inc., California.
- Samson, C. and Ait-Abderrahim, K. 1991a. Feedback control of a nonholonomic wheeled cart in cartesian space. In *Proceedings of the 1991 IEEE International Conference on Robotics and Automation*, Sacramento CA, pp. 1136–1141.
- Samson, C. and Ait-Abderrahim, K. 1991b. Feedback stabilization of a nonholonomic wheeled mobile robot. In *Proceedings of the 1991 IEEE/RSJ International Workshop on Intelligent Robots and Systems*, Osaka, Japan, pp. 1242–1247.
- Schenker, P.S., Huntsberger, T.L., Pirjanian, P., Trebi-Ollennu, A., Das, H., Joshi, S., Aghazarian, H., Ganino, A.J., Kennedy, B.A., and Garrett, M.S. 2000. Robot work crews for planetary outposts: Close cooperation and coordination of multiple mobile robots. In *Proceedings of SPIE Symposium on Sensor Fusion and Decentralized Control in Robotic Systems III*, Boston, MA.
- Seraji, H. 1998. A unified approach to motion control of mobile manipulators. *The International Journal of Robotics Research*, 17(2):107–118.
- Spletzer, J., Das, A.K., Fierro, R., Taylor, C.J., Kumar, V., and Ostrowski, J.P. 2001. Cooperative localization and control for multi-robot manipulation. In *Proceedings of the 2001 IEEE/RSJ International Conference on Intelligent Robots and Systems*, Maui, Hawaii, USA, pp. 631–636.
- Stilwell, D.J. and Bay, J.S. 1993. Towards the development of a material transport system using swarms of ant-like robots. In *Proceedings of the 1993 IEEE/RSJ International Conference on Intelligent Robots and Systems*, Atlanta, GA, pp. 766–771.
- Tang, C.P. 2004. Manipulability-based analysis of cooperative payload transport by robot collectives. M.S. Thesis, University at Buffalo, Buffalo, NY.
- Tang, C.P. and Krovi, V. 2004. Manipulability-based configuration evaluation of cooperative payload transport by mobile robot collectives. In *Proceedings of the 2004 ASME Design Engineering Technical Conferences and Computers and Information in Engineering Conference*, DETC2004-57476, Salt Lake City, UT, USA.
- Tanner, H.G., Kyriakopoulos, K.J., and Krikelis, N.I. 1998. Modeling of multiple mobile manipulators handling a common deformable object. *Journal of Robotic Systems*, 15(11):599–623.
- Wang, Z.-D., Nakano, E., and Matsukawa, T. 1994. Cooperating multiple behavior-based robots for object manipulation. In *1994 IEEE/RSJ International Conference on Intelligent Robots and Systems*.
- Whitney, D.E. 1969. Resolved motion rate control of manipulators and human prostheses. *IEEE Transactions on Man-Machine Systems*, MMS-10:47–53.
- Yamamoto, Y. 1994. Control and coordination of locomotion and manipulation of a wheeled mobile manipulator. Ph.D. Thesis, University of Pennsylvania, Philadelphia, PA.
- Yamamoto, Y. and Yun, X. 1994. Coordinating locomotion and manipulation of a mobile manipulator. *IEEE Transactions on Automatic Control*, 39(6):1326–1332.